# AN AUTOZEROING FLOATING-GATE BANDPASS FILTER

Paul Hasler, Bradley A. Minch, and Chris Diorio

Georgia Institute of Technology
Atlanta, GA 30332-0250,
phasler@ee.gatech.edu

ABSTRACT

We have developed a bandpass floating-gate amplifier that uses tunneling and $p$FET hot-electron injection to set its DC operating point adaptively. Because the gate currents are small, the circuit exhibits a high-pass characteristic with a cutoff frequency less than 1 Hz. The high-frequency cutoff is controlled electronically, as is done in continuous-time filters. We have derived analytical models that completely characterize the amplifier and that are in good agreement with experimental data. This autozeroing floating-gate amplifier demonstrates how to use continuous-time, floating-gate adaptation in amplifier design.

We previously introduced the autozeroing floating-gate amplifier (AFGA)[1]; here, we use the AFGA as an integrated continuous-time bandpass filter. Figure 1 shows the autozeroing floating-gate amplifier. The open-loop amplifier consists of a $p$FET input transistor and an $n$FET current source. With capacitive feedback, the input signal is amplified by a closed-loop gain approximately equal to $-\frac{C_1}{C_2}$. We present data from an AFGA fabricated in the $2\mu m$ $n$well Orbit CMOS process available through MOSIS. Typical operating values for $V_{tun}$ were between $33V$ and $42V$; those for $V_{dd}$ were between $6V$ and $12V$. We obtained similar data in the $1.2\mu m$ $n$well Orbit CMOS process, but with typical operating values for $V_{tun}$ between $26V$ and $31V$. For more modern processes, the typical operating voltages will decrease, because of thinner gate oxides and higher dopant impurity concentrations.

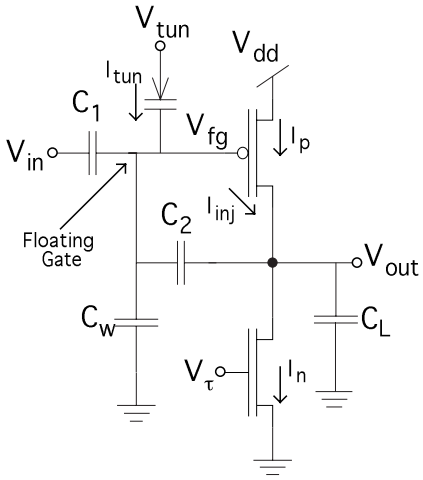


Figure 1: An autozeroing floating-gate amplifier (AFGA) that uses $p$FET hot-electron injection. The ratio of $C_2$ to $C_1$ sets the gain of this inverting amplifier. The $n$FET is a current source, and it sets the current through the $p$FET. Steady state occurs when the injection current is equal to the tunneling current. The capacitances, $C_w$ and $C_L$, represent both the parasitic and the explicitly drawn capacitances. Between $V_{tun}$ and $V_{fg}$ is our symbol for a tunneling junction, which is a capacitor between the floating-gate and an $n$well.

## 1. TIME-DOMAIN AFGA RESPONSE

The complementary $n$FET and $p$FET currents adjust the output voltage such that the amplifier's floating-gate voltage returns to its steady-state value on an intermediate time scale. This circuit behavior translates to a low-pass filter with a short time constant at the output voltage. The quiescent source current ($I_{s0}$) is set by the $n$FET current source. We model the $n$FET transistor as an ideal current source setting the bias current, $I_{so}$, for the AFGA. We describe the channel current of the $p$FET by

$$I_p = I_{so} \exp\left(\frac{-\kappa \Delta V_g}{U_T}\right), \qquad (1)$$

where $\kappa$ is the fractional change in the $p$FET surface potential due to a change in $\Delta V_g$, and $U_T$ is the thermal voltage, $\frac{kT}{q}$. We showed previously that for our operating conditions the AFGA's open-loop gain also is large ($\approx$ 1000) and nearly constant [2]. Since the output capacitances are charged or discharged by currents on the scale of $I_{s0}$, the cutoff frequency will be directly dependent on the bias current. Continuous-time integrators operate on a similar principle [3, 4].

The complementary tunneling and hot-electron injection processes adjust the floating-gate charge such that the amplifier's output voltage returns to its steady-state value on a slow time scale. The combination of electron tunneling and $p$FET hot-electron injection applies the appropriate negative feedback to stabilize the output voltage. If the output voltage is below its equilibrium value, then the injection current exceeds the tunneling current, decreasing the charge on the floating gate; that, in turn, increases the

0-7803-4455-3/98/$10.00 (c) 1998 IEEE

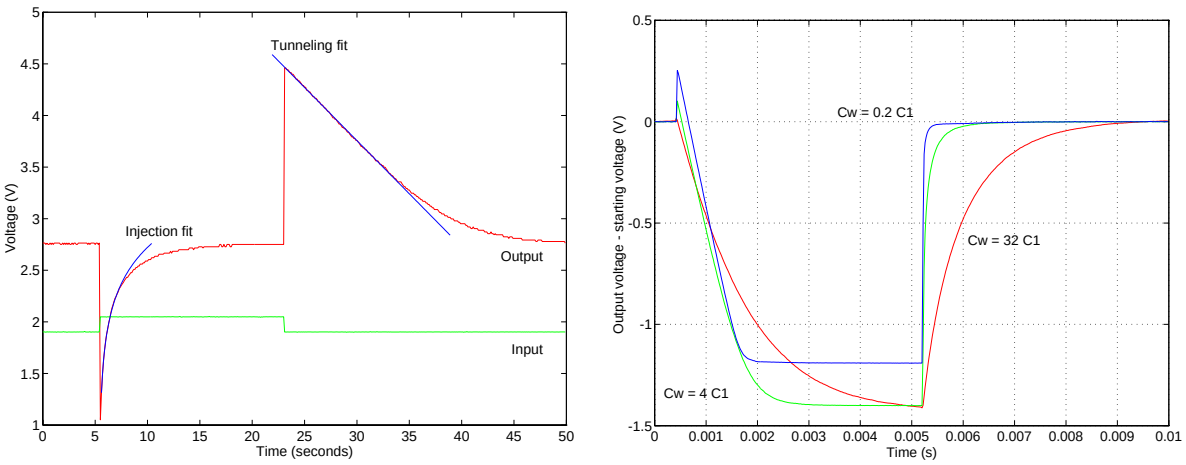


(a) (b)

Figure 2: Response of the AFGA to an upgoing and downgoing step input at two different timescales. (a) The response of an AFGA with a 11.2 bandpass gain to square-wave input at long timescales. The adaptation in response to an upward step results from electron tunneling; the adaptation in response to a downward step results from $p$FET hot-electron injection. We plot the curve fits to highlight the regions where either tunneling or injection dominates the restoration process; $\tau$ is $4.3s$ and $I_{tun0}$ is $50fA$. Decreasing (or increasing) the tunneling voltage decreases (or increases) the adaptation rate; the value of $\tau$ can be set reliably to more than $10^5$ seconds. (b) The response of three unity-gain AFGAs to the same square-wave input at short timescales. All three AFGAs were identical except for their values of $C_w$, and were biased by the same $V_\tau$. Increasing $C_w$ increases the linear range, decreases the amount of capacitive feedthrough, and decreases the low-pass cutoff frequency.

output voltage back toward its equilibrium value. If the output voltage is above its equilibrium value, then the tunneling current exceeds the injection current, increasing the charge on the floating gate; that, in turn, decreases the output voltage back toward its equilibrium value. Since the tunneling and injection currents are many orders of magnitude smaller than $I_{so}$ and are charging similar-sized capacitances, we assume the typical AFGA operating condition that the two timeconstants are sufficiently separated.

### 1.1. Long timeconstant dynamics

The AFGA achieve a high-pass characteristic at frequencies well below 1Hz. To model the low frequency behavior, we first need to describe and model the electron-tunneling and hot-electron–injection processes that generate the floating-gate currents. Our previous papers show that the following expression for the difference of electron-tunneling current ($I_{tun}$) and pFET hot-electron–injection current ($I_{inj}$) is sufficient to model the AFGA effects for a fixed current source [1, 2]:

$$I_{tun} - I_{inj} = I_{tun0}\left(1 - \exp\left(-\frac{\Delta V_{out}}{V_{inj}}\right)\right), \qquad (2)$$

where $V_x$ is a tunneling parameter related to the quiescent tunneling and floating-gate voltages, $V_{inj}$ is an injection parameter related to the quiescent drain and floating-gate voltages, $\Delta V_d$ is the change in the drain voltage around its quiescent value. For our operating conditions in the $2.0\mu m$ Orbit process, a typical value of $V_x$ is $1V$ and of $V_{inj}$ is $250mV$. We define the quiescent injection current must equal the quiescent tunneling current, $I_{tun0}$, at equilibrium. Since the floating gate is held nearly constant by feedback, the floating-gate voltage dependence in (2) is negligible.

We model the low-frequency AFGA behavior by equating the total floating-gate current—the sum of the capacitive currents of the input and output terminals, plus the tunneling and injection currents—to zero. Since the amplifier feedback fixes the floating gate voltage, we get

$$C_2\frac{dV_{out}}{dt} = -C_1\frac{dV_{in}}{dt} + I_{tun0}\left(e^{-\Delta V_{out}/V_{inj}} - 1\right). \qquad (3)$$

If we apply an input voltage step such that $\Delta V_{out}$ moves to $\Delta V_{out}(0^+)$, then we can model how $\Delta V_{out}$ varies with time (t) immediately following this step:

$$\Delta V_{out}(t) = V_{inj}\ln\left(1 + \left(e^{\Delta V_{out}(0^+)/V_{inj}} - 1\right)e^{-t/\tau_l}\right), \qquad (4)$$

where $\tau_l = C_2 V_{inj}\ /\ I_{tun0}$; note that $\Delta V_{out} \to 0$ as $t \to \infty$. Figure 2a shows a measured response to an input pulse, with curve fits highlighting the regions where either the tunneling or injection current dominates.

### 1.2. Short timescale dynamics

To model the high-frequency AFGA behavior, we write two equations governing the autozeroing floating-gate amplifier behavior around an equilibrium output voltage. We obtain the first equation by applying Kirchoff's current law (KCL) at the floating gate (negligible tunneling and injection currents):

$$C_T\frac{dV_{fg}}{dt} = C_1\frac{dV_{in}}{dt} + C_2\frac{dV_{out}}{dt}, \qquad (5)$$

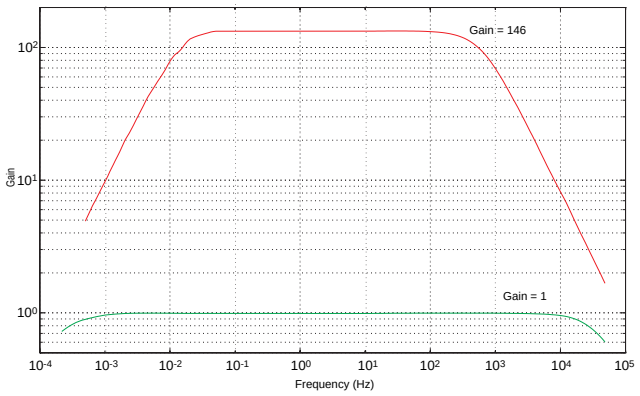


Figure 3: Frequency response for two AFGAs with different gains. For both the high- and low-gain AFGA, $C_1 + C_2$ is approximately constant. For the high-gain AFGA, $\tau_l$ is 20mHz, and $\tau_h$ is 600Hz; for the low-gain AFGA, $\tau_l$ is 300$\mu$Hz and $\tau_h$ is 40kHz. The ratio of $\tau_h$ and $\tau_l$ between the two AFGAs are equal to one-half of the ratio of the gains; the ratio is consistent with a constant $C_1 + C_2$.

where $C_T$ is the total capacitance connected to the floating gate ($C_T = C_1 + C_2 + C_w$). We obtain the second equation by applying KCL at the output node and assuming a sufficiently large open-loop gain:

$$C_o \frac{dV_{out}}{dt} = C_2 \frac{dV_{fg}}{dt} + I_\tau \left( e^{-\kappa \Delta V_{fg}/U_T} - 1 \right). \quad (6)$$

where $C_o$ is the total capacitance connected to the output node ($C_o = C_2 + C_L$), and $\Delta V_{fg}$ is the change in the floating-gate voltage from the quiescent floating-gate voltage. Combining (5) and (6) results in the following equation:

$$\tau_h \frac{dV_{fg}}{dt} = A_h \tau_h \frac{dV_{in}}{dt} + \left( e^{-\kappa \Delta V_{fg}/U_T} - 1 \right), \quad (7)$$

where we define $\tau_h = \left( (C_T C_o - C_2^2)/U_T \right) / (\kappa C_2 I_\tau)$, and $A_h = C_1 / \left( C_T - (C_2^2/C_T) \right)$. The gain from input to output due to capacitive feedthrough is $A_h$. This equation and its solutions are similar to (3).

Figure 2b shows the measured AFGA output-voltage response of a unity-gain AFGAs to a same square-wave input. As in the low-frequency case, the high-frequency response of the AFGA is asymmetric: the downgoing step response approaches its steady state linearly with time, and the upgoing step response approaches its steady state logarithmically with time. The initial jump in the downgoing step is due to capacitive feedthrough. Increasing $C_w$ or $C_L$ without changing $C_1$ and $C_2$ decreases the amount of capacitive feedthrough, and increasing $C_w$ without changing $C_1$ and $C_2$ increases the AFGA's linear range.

## 2. FREQUENCY RESPONSE OF THE AFGA

The AFGA transfer function is bandpass, with the low-frequency cutoff set by the equilibrium tunneling and injection currents, and the high-pass cutoff independently set by the equilibrium $p$FET and $n$FET channel currents. Figure 3 shows the measured AFGA frequency response. From our analysis and data, the AFGA always is a first-order system, even in the presence of parasitic capacitances.

In the adaptation regime, the AFGA behaves as a high-pass filter; the timescale is set by the tunneling and injection currents. We derive the frequency response by keeping only the linear terms when we expand the exponentials in (3) and take the Laplace transform:

$$\frac{V_{out}(s)}{V_{in}(s)} = -\frac{C_1}{C_2} \frac{s\tau_l}{1 + s\tau_l}. \quad (8)$$

The difference between the tunneling voltage and the pFET's floating gate voltage sets the equilibrium tunneling current, $I_{tun0}$, and sets the resulting corner frequency. For moderate tunneling currents, the low-frequency time constant can remain nearly constant for timescales measured in years; any shift is due primarily to trapping in the tunneling oxide.

In the integrating regime, the AFGA behaves as a low-pass filter; the timescale is set by the $n$FET bias current. Again, we derive the frequency response by keeping only the linear terms when we expand the exponentials in (7) and take the Laplace transform:

$$\frac{V_{out}}{V_{in}} = -\frac{C_1}{C_2} \frac{1 - A_h \tau_h s}{1 + \tau_h s}. \quad (9)$$

This transfer function includes the effects of parasitic and load capacitances. The nFET current source sets the bias current and sets the resulting corner frequency. For timescales between the adaptation and integrating regimes, the AFGA acts as an amplifier. At frequencies much higher than the integrating regime, the AFGA exhibits capacitive feedthrough (not seen in Fig. 3), which can be reduced by an increase in either $C_w$ or $C_L$.

## 3. LINEAR RANGE, NOISE, AND DYNAMIC RANGE

Our criterion for linearity is that $\Delta V_{fg}$ be sufficiently small that the factor $\left( \exp\left( -\frac{\kappa \Delta V_{fg}}{U_T} \right) - 1 \right)$ in (7), can be approximated by $-\frac{\kappa \Delta V_{fg}}{U_T}$. This criterion implies that the floating-gate voltage must not move by more that $\frac{U_T}{\kappa}$ from its equilibrium value. The floating-gate voltage has its maximum swing in the capacitive-feedthrough regime; therefore, the input linear range, $V_{Li}$, and the output linear range, $V_{Lo}$, are

$$V_{Li} = \frac{U_T}{\kappa} \left( \frac{C_T}{C_1} \right) B, V_{Lo} = \frac{C_1}{C_2} V_{Li} = \frac{U_T}{\kappa} \left( \frac{C_T}{C_2} \right) B, \quad (10)$$

where we define $B = 1 - C_2^2 \; / \; C_T C_o$. In typical operation, $B$ is a correction term nearly equal to 1 [2]. By increasing $C_w$, we can reduce the change in the floating-gate voltage, thereby increasing the amplifier's output linear range. For a sufficiently large open-loop gain, the AFGA's passband gain is independent of $C_w$. Figure 4 shows measured data demonstrating how $\tau_h$ and linear range scale with $C_w$ for unity-gain AFGAs. For a unity-gain AFGA—that is for $C_1 = C_2$—the expressions for $\tau_h$ and input linear range are

$$\tau_h = \frac{1.5 U_T C_1}{\kappa I_\tau} \left( 1.5 + \frac{C_w}{C_1} \right), V_{Li} = \frac{U_T}{\kappa} \left( 1.5 + \frac{C_w}{C_1} \right). \quad (11)$$

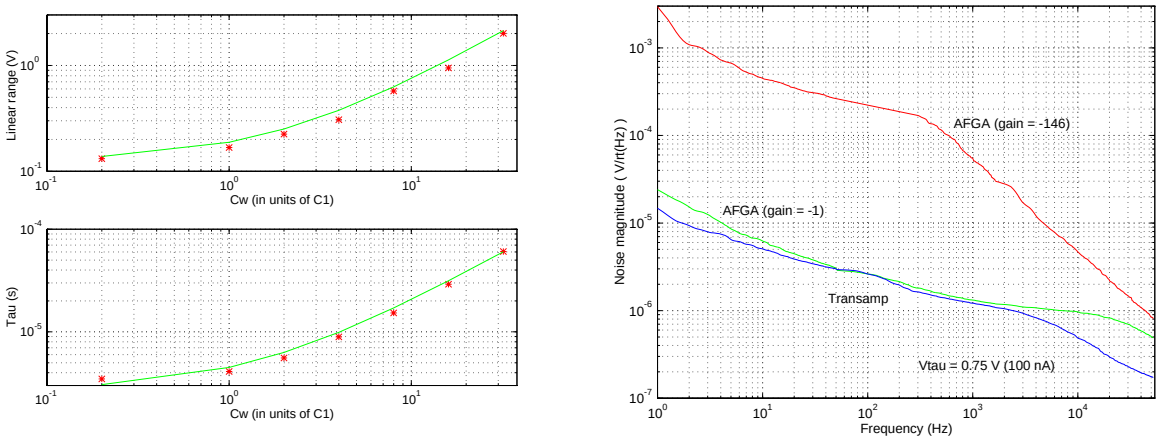


(a) (b)

Figure 4: (a) Measured linear range and $\tau_h$ for several unity-gain AFGAs for different $C_w$ ratioed in units of $C_1$. The linear range fit is $V_{Li} = 0.063\text{V}\ C_w/C_1 + 0.094\text{V}$, and the *tau* fit is $\tau = 1.8\mu\text{s}\ C_w/C_1 + 2.7\mu\text{s}$. (b) Noise spectrum of an AFGA for a constant input. The spectrum was taken for a bias current of $80nA$, which corresponds to a $V_\tau$ of $0.73V$. Comparison of a high-gain AFGA with a unity-gain AFGA and with a generic follower-connected differential amplifier. All three amplifiers had the same $V_\tau$ voltage, and had the same bias current. The sums of $C_1$ and $C_2$ are the same for the two AFGAs.

where measured $C_L$ is approximately $C_1$.

Both from experimental data and from the direct analytic solution of (7), second harmonic distortion dominates for the AFGAs; for a sine-wave input with amplitude of $V_{Li}$, the peak second harmonic distortion is 0.05 percent of, or 26dB below, the fundamental frequency response. The second harmonic distortion is maximum for frequencies just below $\frac{1}{2\pi\tau_h}$; for amplitudes at or below $V_L$, the second harmonic distortion is proportional to the square of the fundamental amplitude.

MOS devices and quantum processes, such as electron tunneling and hot-electron injection, are often criticized for their high $1/f$ noise. Figure 4b shows a comparison among a high-gain AFGA, a unity-gain AFGA, and a follower-connected transconductance amplifier for a fixed, voltage-source input—that is, the output-voltage noise from the amplifier. Both AFGAs used the same constant tunneling current levels. The transconductance amplifier is the wide-range amplifier described previously [4]; it has transistors larger than those of the AFGAs, resulting in the lower $1/f$ noise. Since the AFGA's noise performance is similar in thermal and $1/f$ characteristics to that of a standard MOS amplifier, we conclude that the tunneling and injection processes do not add appreciable noise to the amplifier.

We define dynamic range, DR, as the ratio of the maximum possible linear output swing to the total output-noise power. We derive elsewhere that the total output-noise power as [2]

$$\hat{V}_{out}^2 = \left(\frac{C_T}{C_2 g_m}\right)^2 \int_0^{\frac{2\pi}{\tau_h}} \frac{\hat{i}_o^2}{1+(\omega\tau_h)^2}\frac{df}{\Delta f} = \frac{qU_T}{\kappa B}\frac{C_T}{C_2 C_o}. \tag{12}$$

The total output-noise power is roughly proportional to $C_w$, and is inversely proportional to $C_L$. We can express the AFGA dynamic range (DR) as

$$DR = \frac{V_{Lo}^2}{2\hat{V}_{out}^2} = \frac{\kappa}{2q} V_{Lo} C_o B^2, \tag{13}$$

which is similar to the form for dynamic range for the wide-linear-range amplifier, as derived in [5]. The dynamic range varies inversely with $C_2$; therefore a high-gain amplifier will have a larger dynamic range than will the low-gain amplifier for the same values of $C_1$, $C_w$, and $C_L$. In summary, we can increase the linear range by increasing $C_w$, and we can increase the dynamic range by increasing $C_w$ or $C_L$.

## 4. REFERENCES


[1] P. Hasler, B.A. Minch, C. Diorio, and C. Mead, "An autozeroing amplifier using $p$FET hot-electron injection", Proceedings of the International Symposium on Circuits and Systems, Atlanta, vol.3, 1996, pp. 325-328. Also at http://www.ee.gatech.edu/users/phasler

[2] P. Hasler, B.A. Minch, C. Diorio, and C. Mead, "An autozeroing floating-gate amplifier", Circuits and Systems II: Digital and Analog Signal Processing, in Press.

[3] Y. Tsividis, M. Banu, and J. Khaury, "Continuous-time MOSFET-C filters in VLSI", IEEE Transactions on Circuits and Systems, vol.33, no.2, 1986

[4] C. Mead, Analog VLSI and Neural Systems, Addison - Wesley, Reading, MA, 1989.

[5] R. Sarpeshkar, R. F. Lyon, and C. Mead, "A low-power wide-linear-range transconductance amplifier," Analog Integrated Circuits and Signal Processing, vol. 13, no. 1/2, 1996, pp.123-152.